

Parameter Symmetry Breaking and Restoration Determines the Hierarchical Learning in AI Systems

Liu Ziyin^{1,3}, Yizhou Xu², Tomaso Poggio¹, Isaac Chuang¹

¹*Massachusetts Institute of Technology*
²*École Polytechnique Fédérale de Lausanne*
³*NTT Research*

February 11, 2025

Abstract

The dynamics of learning in modern large AI systems is hierarchical, often characterized by abrupt, qualitative shifts akin to phase transitions observed in physical systems. While these phenomena hold promise for uncovering the mechanisms behind neural networks and language models, existing theories remain fragmented, addressing specific cases. In this paper, we posit that parameter symmetry breaking and restoration serve as a unifying mechanism underlying these behaviors. We synthesize prior observations and show how this mechanism explains three distinct hierarchies in neural networks: learning dynamics, model complexity, and representation formation. By connecting these hierarchies, we highlight symmetry – a cornerstone of theoretical physics – as a potential fundamental principle in modern AI.

1 Introduction

More and more phenomena that are virtually universal in the learning process have been discovered in contemporary AI systems. These phenomena are shared by models with different architectures, trained on different datasets, and with different training techniques. The existence of these universal phenomena calls for one or a few universal explanations. However, until today, most of the phenomena are instead described by narrow theories tailored to explain each phenomenon separately – often focusing on specific models trained on specific tasks or loss functions and in isolation from other interesting phenomena that are indispensable parts of the deep learning phenomenology. Certainly, it is desirable to have a *universal perspective*, if not a *universal theory*, that explains as many phenomena as possible. In the spirit of science, a universal perspective should be independent of system details such as variations in minor architecture definitions, choice of loss functions, training techniques, etc. A universal theory would give the field a simplified paradigm for thinking about and understanding AI systems and a potential design principle for a new generation of more efficient and capable models.

Learning phenomena in deep learning can be roughly categorized into three types, each capturing a different kind of hierarchy hidden in neural networks:

- **Hierarchy of Learning Dynamics:** distinct *temporal* regimes arise during learning – this includes abrupt complexity jumps (Simon et al., 2023; Jacot et al., 2021; Abbe et al., 2023), progressive sharpening and flattening (Cohen et al., 2021), and beyond-linear dynamics of training (Zhu et al., 2022);
- **Hierarchy of Model Complexity:** the *functional* complexity of models adapts to the target function – this is exhibited in simplicity biases (Kalimeris et al., 2019), compressive coding through the information bottleneck (Tishby et al., 2000; Tishby & Zaslavsky, 2015), and the “blessing of dimensionality” in overparameterized nets (Galanti et al., 2021; Zhang et al., 2017);
- **Hierarchy of Neural Representation:** distinct *spatial* structures arise in the layers of neural networks, with progressively deeper layers tending to encode increasingly abstract information – this is evidenced in the structured representations such as neural collapse (Papayan et al., 2020), hierarchical encoding of

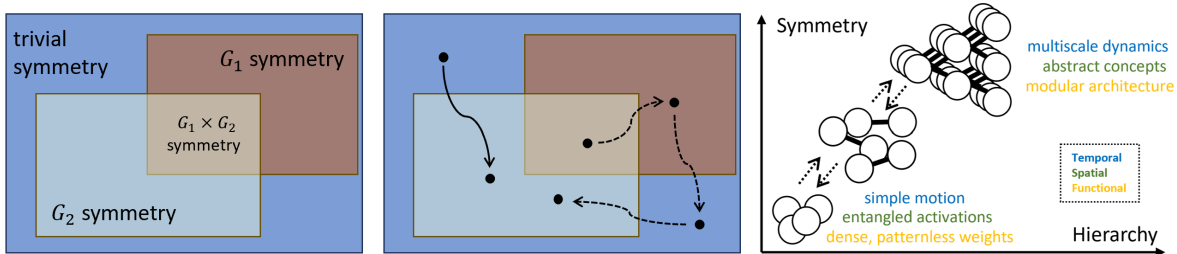


Figure 1: The division of solution space into hierarchies given by distinct parameter symmetries. **Left:** Example solution space of a model with parameter symmetries can be divided into hierarchies with boundaries prescribed by symmetry-breaking conditions. The more symmetry there is, the more restricted the hypothesis space becomes. **Middle:** The temporal (learning dynamics) and spatial (layer-wise information processing) dynamics of AI models can be characterized by the transitions between different symmetry groups. The solid line shows a symmetry restoration dynamics when the parameter transitions from a low-symmetry state to a high one either through time or through layers. The dashed lines show compositional dynamics where the model follows two symmetry breaking and then a symmetry restoration. Actual learning dynamics of neural networks may involve the model first learning by breaking symmetries before regularization effects dominate (Li et al., 2021), restoring symmetry. Similarly, for spatial processing, neural networks are found to break symmetries in early layers and restore symmetries in final layers (Section 5). **Right:** The more symmetry a model has, the more spatial, temporal, and functional hierarchies it has. Changes in symmetries can induce transitions between these hierarchies.

features (Zeiler & Fergus, 2014), and universal alignment of representations across models (Huh et al., 2024).

In this paper, we posit that these three seemingly unrelated hierarchies of deep learning phenomena can be collectively understood as arising from a single concept regarding the behavior of model parameter symmetries during training:

Main Hypothesis: The hierarchies of learning dynamics, model complexity, and representation formation in AI systems are primarily determined by parameter symmetry breaking and restoration.

Prior art has certainly hinted at this idea, but here we draw together many separate threads to complete a single picture, as illustrated in Figure 1. The main idea is that parameter symmetry (defined in Section 2) divides the solution space into hierarchies, such that three key effects result:

- *Temporal* jumps follow transitions between symmetry groups (Section 3);
- *Functional* constraints arise adaptively along boundaries of symmetry (Section 4);
- *Spatial* hierarchy of abstract representations arise due to layered symmetries (Section 5).

Given parameter symmetry as a unifying mechanism for deep learning, our understanding of the principles of AI can advance with explicit identification and engineering of symmetries in models, loss functions, and data. With the recent advances in how arbitrary parameter symmetries may be deliberately introduced or removed (Section 6), it is now possible to design symmetries matching practitioner intentions. Moreover, given widespread beliefs that hidden hierarchy phenomena of the kinds described above are beneficial, it follows one should be able to design models with intentional symmetries to introduce hierarchies into learning dynamics, the learned function complexities, and the layered structure of neural networks.

The next section introduces parameter symmetry. We then discuss existing supports for the three specific hypotheses given above. Section 6 discusses mechanisms that cause and methods for controlling symmetry breaking and restoration. The last section discusses alternative views. Formal theorems, experimental details, and additional figures are presented in the appendix.

2 Parameter Symmetry in Deep Learning

Definition 1. Let G be a linear representation of a group. We say that there is a G -parameter symmetry in the model $f(\theta, x)$ if $\forall g \in G$ and $\forall x$, $f(\theta, x) = f(g\theta, x)$.

Symmetry	Model condition	Symmetric State	Example
translation	$f(w) = f(w + \lambda z)$ for fixed z	none	softmax, low-rank inputs
scaling	$f(w) = f(\lambda w)$	none	batchnorm, etc.
rescaling	$f(u, w) = f(\lambda u, \lambda^{-1} w)$	$\ u\ = \ w\ $	ReLU neuron
rotation	$f(W) = f(RW)$ for orthogonal R	low-rank solutions	self-supervised learning
permutation	$f(u, w) = f(w, u)$	identical neurons	fully connected layers, ensembles
double rotation	$f(U, W) = f(UA, A^{-1}W)$	low-rank solutions	self-attention, matrix factorization
sign flip	$f(w) = f(-w)$	$w = 0$	tanh neuron

Table 1: Common parameter symmetries in deep learning. We divide θ into three parts: $\theta = (w, u, v)$, where w and u are related to symmetry, while v is symmetry-irrelevant and is omitted. Note that these symmetries are not mutually exclusive. For example, double rotation or rotation symmetry implies permutation symmetry and sign flip. Double rotation also implies rescaling. Some continuous groups do not have a discrete subgroup, such as the scaling and translation symmetry, which is also included for completeness. However, they still interact with regularizations in an interesting way: If there is a weight decay, the global minima are achieved at zero, which is ill-behaved for scaling symmetry but not for translation. Also, note that Z_2 subgroups are particularly common in these symmetries.

Definition 2. Let $P_G = \frac{1}{|G|} \sum_{g \in G} g$. The model parameter θ is said to be in a G -symmetric state if $P_G \theta = \theta$. Otherwise, θ is in the symmetry-broken state.

P_G is the projection matrix to the symmetry-invariant subspace of G (Feit, 1982). Note that if $P_G \theta = \theta$, then $g\theta = \theta$ for any g because $gP_G = P_G$. A striking fact for those unfamiliar with parameter symmetries is that many such parameter symmetries exist in widely used loss functions and neural networks (see Table 1). Understanding the implications of such symmetries has been an active area of research (Simsek et al., 2021; Entezari et al., 2021; Dinh et al., 2017; Saxe et al., 2013; Neyshabur et al., 2014; Tibshirani, 2021; Ioffe & Szegedy, 2015; Zhao et al., 2023b; Godfrey et al., 2022), and this has been challenging since the number of groups induced by these symmetries often grows exponentially in the size of the model. Many prior works have explored the effect of parameter symmetry on constraining the model complexity or learning dynamics (Li et al., 2016; Saxe et al., 2013; Du et al., 2018; Tanaka & Kunin, 2021; Zhao et al., 2022; Marcotte et al., 2023; Li et al., 2020). Because parameter symmetry naturally means that part of the solution space is redundant, having parameter symmetry can be seen as a form of “overparameterization.”

Example: Consider the parameter symmetries in the self-attention logit of a transformer, which can be written as (using notation from Vaswani et al. (2017))

$$a_{ij}(W_Q, W_K) = X_i^T W_Q W_K X_j. \quad (1)$$

It has a double rotation symmetry: for any invertible M , $a_{ij}(W_Q M, M^{-1} W_K) = a_{ij}(W_Q, W_K)$, which implies that the loss function is also invariant to this transformation. This, in turn, implies that the symmetric states are those with low-rank W_Q and W_K . Note that a_{ij} can also be written as

$$a_{ij}(W_Q, W_K) = X_i^T \sum_l W_Q^l (W_K^l)^T X_j, \quad (2)$$

where W_Q^l is the l -th column of W_Q and W_K^l is the l -th row of W_K . This means that it also has the permutation symmetry such that for any l and l' , $a_{ij}(W_Q^l, W_K^l, W_Q^{l'}, W_K^{l'}) = a_{ij}(W_Q^{l'}, W_K^{l'}, W_Q^l, W_K^l)$. An alternative way to see this is that permutation symmetry is a subgroup of the double rotation symmetry (because permutation matrices are invertible). For each l , there is also the sign flip symmetry, $a_{ij}(W_Q^l, W_K^l) = a_{ij}(-W_Q^l, -W_K^l)$, and the rescaling symmetry, $a_{ij}(\lambda W_Q^l, \lambda^{-1} W_K^l)$. Note that if X is low-rank in the z -direction, these matrices also have a translation symmetry, where $a_{ij}(W_K^l + \lambda z) = a_{ij}(W_K^l)$ for any l and $\lambda \in \mathbb{R}$. Therefore, we have seen that even for a single self-attention layer, there are many symmetries. Note that these symmetries are independent of the data distribution and apply to every pair of X_i and X_j – this is the main reason these symmetries could significantly affect training neural networks. Recent works have shown that double rotation symmetry causes the self-attention layers to have a low-rank bias (Kobayashi et al., 2024).

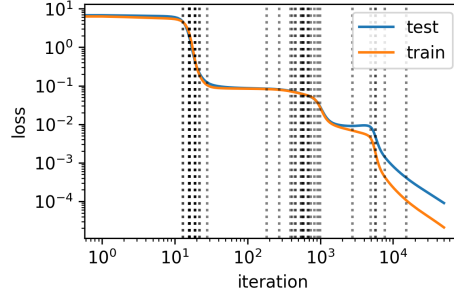


Figure 2: DNN learning dynamics is symmetry-to-symmetry. Recent works suggested the learning of neural networks is primarily saddle-to-saddle (Jacot et al., 2021), and escaping these saddle points coincides with a sudden change in the complexity of the network (Abbe et al., 2023). At the same time, symmetries have been found to be the primary causes of the saddle points (Li et al., 2016; Ziyin, 2024). Once the symmetry is removed, saddle points seem to have disappeared when interpolating different solutions of the model (Lim et al., 2024). The figure shows that the loss jumps when symmetry breaking happens (black dotted lines) and plateaus when there is no symmetry breaking.

3 Learning Dynamics is Symmetry-to- Symmetry

Symmetry has a direct influence on the loss landscape, and it thus affects the learning dynamics of neural networks through its effect on the landscape (Tatro et al., 2020; Lim et al., 2024). One primary effect of symmetry on the loss landscape is that it creates extended saddle points from which SGD or GD cannot escape (Li et al., 2016; Chen et al., 2023). Meanwhile, it has been found that when a neural network is initialized with small norm weights, its learning dynamics is primarily saddle-to-saddle (Jacot et al., 2021). In fact, neural networks have been found to converge often to saddle points (Alain et al., 2019; Ziyin et al., 2023). Given that symmetries are the primary origins of saddle points, it is natural to hypothesize that the learning dynamics of neural networks are not only saddle-to-saddle but symmetry-to-symmetry:

Dynamics Hypothesis: The learning dynamics of neural networks are dominated by jumps between symmetry groups, with parameters going from a larger to a smaller group (symmetry breaking) or from a smaller to a larger group (restoration).

As Theorem 1 in the next section shows, at a G -symmetric solution, the number of effective model parameters is reduced by a number that matches the rank of the group. This means the change between symmetries naturally induces a change in model complexities. Therefore, these symmetry-to-symmetry jumps not only in terms of the loss function value but also in terms of complexity jumps.

Definition 2 can quantify the breaking and restoration of symmetry. We define the symmetry-breaking distance as:

$$\Delta^G = \|\theta - P_G \theta\|_2^2. \quad (3)$$

When $\Delta^G > \Delta_{\text{th}}^G$ for some threshold Δ_{th}^G ($\Delta_{\text{th}}^G = 0.05 \sim 0.2$ in experiments), we say the G -symmetry is broken. We care about how many symmetries are broken for a given layer, so we can count the number of such large Δ^G . For example, for permutation symmetry in a fully connected layer, the group-invariant projection is the average of the input and output weights of any pair of neurons i and j . One can identify each pairwise distance as a different Δ^G , which we will denote as Δ_{ij}^G throughout this work. We only need to count the number of neighboring neurons with a large Δ^G because they form a generating set of the symmetric group – we refer to this number as the *degree of symmetry* N_{dos} . The difference between N_{dos} and the number of neurons is the *degree of symmetry breaking* (N_{dosb}). See Section A.1 for details on measuring this quantity.

Figure 2 shows an example where we train an MLP in a teacher-student setting using SGD. We initialize the model at a small norm, so the model’s initial state is approximately in the symmetric state, where the average pairwise distance is of order 10^{-4} . The black dashed lines show when a pairwise distance exceeds Δ_{th}^G , signaling a symmetry breaking. We see that the symmetry-breaking times coincide well with the periods where the network learns rapidly. This shows that the saddle-to-saddle learning dynamics is potentially caused by the symmetry-to-symmetry transitions during training. Examples with polynomial and sinusoidal nets are shown in Section A.2.

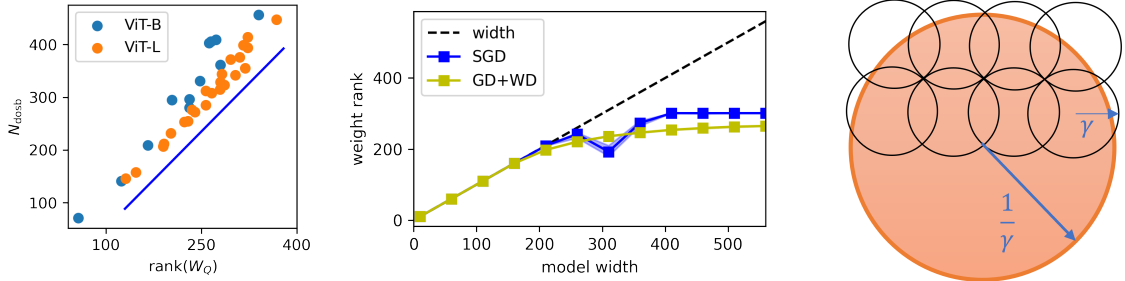


Figure 3: The complexity and generalization error of neural networks do not grow with width. A well-known observation in deep learning is that overparameterized networks not only work well, but also their generalization errors are empirically found to be essentially independent of width (Li & Wang, 2018; Pinto et al., 2024; Galanti et al., 2023; Mingard et al., 2025), an observation at odds with conventional bounds based on the Rademacher complexity (Zhang et al., 2017). The existence of parameter symmetries may solve this problem because, with a fixed regularization, the maximum surviving neurons are upper bounded by a constant. The **left** figure shows that Imagenet-pretrained ViT-Base (80M) and ViT-Large (300M) have similar degrees of symmetry in their self-attention layers. Here, each dot is a self-attention layer. The **middle** figure shows that the weight rank does not grow with increasing model size. A mechanism for this is that permutation symmetry implies that neuron weights of distance $o(\gamma)$ to each other must collapse – this means that within a fixed n -sphere, there can be at most $1/\gamma^n$ different neurons. This filling procedure is illustrated in the **right** figure: The orange circle denotes the parameter space, and the little circles are the neuron weights.

Decomposability into Quadratic Models Another interesting point worth raising about symmetries is that if the model is close to a symmetric state θ^* , then it can be decomposed into a sum of a quadratic model and a strictly smaller model. Ziyin (2024) showed that for a small Δ^G ,

$$f(\theta, x) = f(\theta^*) + \theta_G^T \nabla^2 f(\theta^*, x) \theta_G + o(\Delta^G), \quad (4)$$

where $\theta^* = P_G \theta$ is essentially a parameter projected to a $d - \text{rank}(P_G)$ subspace, and $\theta_G = (I - P_G)\theta$ are the parameters projected to the symmetry breaking direction. Therefore, the second term can be seen as a quadratic model trained on a data transformation kernel of the form $\nabla^2 f(x)$. This means that close to symmetry states, the learning dynamics must be “diligent” and cannot be characterized by NTK (Jacot et al., 2018) or lazy training (Chizat et al., 2018). This implies that parameter symmetry also plays a significant role in feature learning (Yang & Hu, 2020). In contrast, if a model has an antisymmetry, its expansion will only have odd order terms, and one may expect that such a model primarily behaves like a linear model.

4 Symmetry Adaptively Limits Model Complexity

Another important implication of symmetries is that they control the effective number of parameters. When a system is symmetry-broken, new degrees of freedom usually emerge (known as a Goldstone mode in physics (Peskin, 2018)), and the system becomes higher-dimensional and more complex. When it is symmetry-restored, the effective dimension is reduced. This means that the symmetry boundaries naturally correspond to boundaries of different hierarchies of model capacities. This idea has a place in machine learning. For example, equivariant networks can improve the sample efficiency of training, and existing equivariant networks almost always involve introducing new parameter symmetry to the neural network (Maron et al., 2018; Bronstein et al., 2021). In Bayesian learning, parameter symmetry (and its generalizations) have been found to directly determine the generalization scaling of the model (Watanabe & Opper, 2010). Prior works also indicate how neural networks may break symmetries to adapt to different tasks (Fok et al., 2017).

More broadly, combining the idea that symmetry classes have different model complexity and the common observation that SGD tends to learn a function whose complexity is proportional to the complexity of the target function (Kalimeris et al., 2019; Mingard et al., 2025), it is natural to arrive at the following hypothesis:

Complexity Hypothesis: Symmetry adaptively controls the model’s capacity. The model converges to a symmetry class whose complexity matches the complexity of the target.

The direct correspondence between symmetry and model capacity has been justified by a recent result: at a G -symmetric state, the effective model dimension decreases by exactly $\text{rank}(P_G)$ throughout training. Moreover, in the NTK limit, this reduction in parameter dimension implies a selection of input features, and being at a symmetric solution directly affects the input-output function map.

Theorem 1. (Informal, (Ziyin et al., 2025b)) *If the loss function has G -symmetry, and the initial $\theta \in \mathbb{R}^d$ is G -symmetric, then (1) there exists a model with $d - \text{rank}(P_G)$ parameters whose learning dynamics is the same as θ , and (2), in the lazy training regime, this is equivalent to applying a rank $d - \text{rank}(P_G)$ mask to the NTK features.*

Thus, symmetric solutions are low-capacity states from which gradient-based training methods cannot escape. More importantly, these symmetric solutions are preferred solutions when weight decay is used (Ziyin, 2024) or if the minibatch noise is strong due to a mechanism called “stochastic collapse” (Chen et al., 2023).

Parameter Symmetry as an Occam’s Razor In other words, parameter symmetries in the model may function like an Occam’s razor, where simpler and low-complexity solutions are favored – an observation that has been made across almost all modern neural models, whose generalization performances are independent of the size of the model (Zhang et al., 2017; Galanti et al., 2023), which is in discrepancy with common generalization bounds that predict a $\sqrt{\psi}$ deterioration with respect to the width ψ (Neyshabur et al., 2018). One can test this hypothesis simply by training an MLP and a small transformer on different randomly generated teacher networks – see Section A.5. For different tasks, the same network converges to solutions with different symmetry classes corresponding to different levels of complexity. Similarly, for a fixed task, networks with different levels of capacity converge to similar degrees of symmetry. See Figure 3-Left for vision transformers (ViT) (Dosovitskiy, 2020) trained on Imagenet.

Here, we raise an insightful conjecture about the quantification of complexity control due to permutation symmetry, where γ is the weight decay, η/S is the learning-rate-batch-size ratio. Recall that the distance between two neurons is Δ_{ij} .

Conjecture 1. (Space Quantization Conjecture, Informal) *In every layer with permutation symmetry, for two nonidentical neurons i and j , $\Delta_{ij} > O(\kappa^\beta)$ after training, where $\beta > 0$ and κ is the regularization strength.*

We prove a special case in Section B.3. A primary mechanism for this absolute upper limit is a combination of regularization and symmetry (Section 6): (1) using weight decay γ , the model parameters must lie within a ball of radius $O(1/\gamma)$ to the origin; (2) with symmetry any neuron whose weights are with a distance of γ to each other must become identical. This means that the number of surviving neurons is upper bounded by the number of n -hyperspheres of radius $O(\gamma)$ that one can fit in a hypersphere of radius $O(1/\gamma)$; this number can be upper bounded by $O(\gamma^{-n})$. This exponential index can be improved to be independent of n and so does not suffer the curse of dimensionality (Section B.3). From a physics picture, the neurons start to form a “lattice” in the parameter space with the lattice distance γ .

Thus, when regularized, there are, at most, a finite number of nonidentical neurons within a layer, however wide it is. This implies that the actual complexity of the trained network must decrease as a function polynomial in the regularization strength. See Figure 3-Middle, where we train a two-hidden-layer network with varying widths. When weight decay or stochastic training is used, we see that the dimension of the latent representation saturates at a large model size. This could imply that the actual model complexity is much smaller than its apparent dimension and may be a key mechanism for understanding why highly overparametrized networks can still generalize. For example, Bartlett et al. (2019) showed that the VC dimension of a two-layer piecewise linear network is $O(\psi)$. Our result implies that the nonidentical number of neurons must be $O(1)$ after training. This, in turn, means that the VC dimension of the model is independent of width.

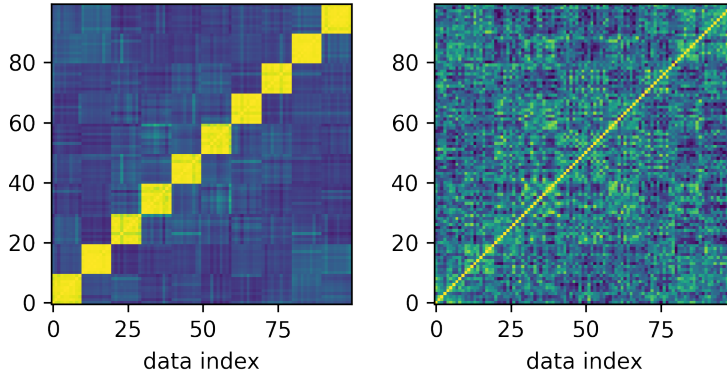


Figure 4: Neural collapse (NC) only happens when permutation symmetry is present. NC is a primary example of how invariant high-level representations emerge in neural networks (Papayan et al., 2020) and exist quite generally in classification, regression, and large language models (Andriopoulos et al., 2024; Wu & Papayan, 2024). When NC happens, the learned representation must be low-rank; however, Ziyin et al. (2025b) showed that if the permutation symmetries are removed, the learned representation is always full-rank. This implies that permutation symmetry is a necessary condition for NC to happen. The figures show the representation alignment of 100 CIFAR10 images across 10 classes (10 images in each class). The color represents the correlation between representations. **Left:** The vanilla model exhibits neural collapse, where all neurons are similar for the same class. **Right:** The innerclass variation becomes significant when the permutation symmetry is removed.

5 Representation Learning Requires Parameter Symmetry

Representation learning is believed to be the most essential aspect of deep learning (Bengio et al., 2013). Learned representations of neural networks are found to take almost universally hierarchical forms, where earlier layers encode a large variety of low-level features and later layers learn a composed and abstract representation that is invariant to the changes in the low-level details (Zeiler & Fergus, 2014). One reason why symmetry may serve as a driving mechanism for learning these structured representations is that these structures almost always involve compressing information onto a few neurons and come with a low-rank structure in the hidden layer (Alain, 2016; Masarczyk et al., 2024; Xu et al., 2023; Papayan et al., 2020), and a primary low-rank mechanism for deep neural networks is through the permutation symmetry of the layer or the rescaling symmetry of ReLU neurons (Fukumizu, 1996; Fukumizu & Amari, 2000; Ziyin, 2024). As a primary example, neural collapses (NC) often happen in an image classification task, where the inner-class variations are found to disappear in the last and intermediate layers of the neural network (Papayan et al., 2020), resulting in a representation whose rank matches the number of classes. This implies that the network has learned a hierarchical representation, where, in the later layers, only high-level features are encoded. These results motivate the following hypothesis:

Representation Hypothesis: Learning invariant, hierarchical and universal latent representations requires parameter symmetry.

Invariant and Hierarchical Representation Learning See Figure 4. Here, we train a standard ResNet18 on CIFAR-10, which is known to exhibit NC. In comparison, we also train a ResNet18 whose symmetries have all been removed using the method proposed in (Ziyin et al., 2025b). We see that after removing permutation symmetries, the innerclass variation of representations no longer vanishes. In Section A.4, we show that the spectral gap between class means and innerclass variations also becomes smaller.

More broadly, it is important to understand how representations build up as the input data passes through layers of a neural network. It seems likely that there are at least three distinctive regimes in the layers of a trained net: the first few layers of neural networks serve as an *expansion* phase where the representation becomes linearly separable (Alain, 2016), which requires the layer to be wide and implies a high rank (Nguyen et al., 2018); then, a “reduction” phase happens where the irrelevant information is thrown away and the neurons encode more and more compact information (Xu et al., 2023; Rangamani et al.,

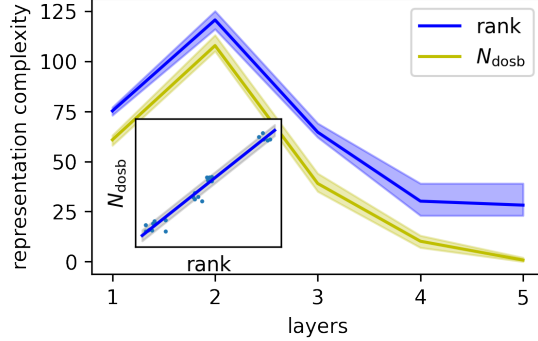


Figure 5: Neural networks learn a hierarchical representation. Recent works on representation learning have suggested that the rank of the latent representation first increases and then decreases through the layers (Xu et al., 2023; Masarczyk et al., 2024). This is reasonable because, on the one hand, a network needs to be wide enough to learn disconnected decision regions (Nguyen et al., 2018), while permutation symmetries drive towards low-rankness (Ziyin, 2024). This figure shows the rank and degree of symmetry breaking, which can be seen as the simplest metrics of the representation complexity, of different layers in a 5-layer FCN trained on CIFAR-10. This experiment shows hierarchical representations may be due to symmetry changes: the beginning layers feature symmetry breaking, and later layers are primarily symmetry restoration.

2023); lastly, a “transmission” phase where the layers do nothing except transmitting the signal it receives (Masarczyk et al., 2024). The NC can be seen as an example of the transmission and the simplest case of such a hierarchical representation (Ziyin et al., 2025a). These results all suggest that the representation rank is a good metric of the complexity of the layer. As Figure 5 shows, these changes in the representation ranks match well the symmetry-breaking level of the layer, a strong evidence that symmetry may drive the formation of hierarchical representations.

Universal Representation Learning The neural collapse is also a special case of what we will call “universal representation learning.” Recent works found that the representations of learned models are found to be universally aligned to different models trained on similar datasets (Bansal et al., 2021; Kornblith et al., 2019), and to the biological brains (Yamins et al., 2014). This interesting phenomenon has a rather philosophical undertone and has been termed “Platonic Representation Hypothesis” (Huh et al., 2024). Here, we say that the two neural networks have learned a universal representation if for all x_1, x_2 ,

$$h_A(x_1)^T h_A(x_2) = h_B(x_1)^T h_B(x_2), \quad (5)$$

where h_A is the normalized activation of network A in one of the hidden layers, and h_B for network B . This is an idealization of what people have observed – and the difference between the two sides is the “degree of alignment”. The NC is a special case because when NC happens, the representations form a simplex tight frame, and so two networks with NC must have an aligned representation.

Recent results have suggested that symmetry may play a key role in shaping the representation of neural networks. The following theorem can be proved by leveraging Theorem 5.4 of Ziyin et al. (2024), which shows that the double rotation symmetry in deep linear networks leads to the emergence of universal representations in different models, even when data and models are different.

Theorem 2. (Informal) Let $\mathcal{D}_M = \{(Mx_i, y_i)\}_i$ be the training set, where M is an invertible matrix. Let deep linear networks A and B have arbitrary depths and widths. Let model A train with SGD on \mathcal{D}_M and model B with SGD on $\mathcal{D}_{M'}$, for arbitrary M, M' . Then, if the model converges and is at the global minimum, every layer h_A of A is **perfectly** aligned with every layer h_B of B for any x :

$$h_A(x) \propto R h_B(x), \quad (6)$$

where R is an orthogonal matrix.

See Figure 6. This is an extraordinary fact: due to the double rotation symmetry, there exist infinitely many global minima for a deep linear network such that the representations are not aligned. Yet, SGD training finds a special solution such that every layer of A is aligned with every layer of B despite having

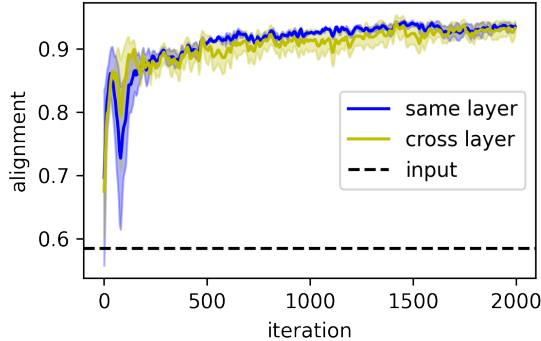


Figure 6: Universally aligned representations emerge in differently trained neural networks. Many recent works demonstrate that different trained neural networks learn representations that are similar to each other and even to the biological brain (Huh et al., 2024; Kornblith et al., 2019; Yamins et al., 2014). Parameter symmetry may be a core mechanism for this intriguing phenomenon as it implies a universal alignment between representations (Ziyin et al., 2024). The figure shows the representations of two deep linear networks independently trained on randomly transformed MNIST become perfectly aligned for **every** pair of layers. The figure shows the average alignment between the same or different layers of two networks. This alignment does not weaken even if the input is arbitrarily transformed (Theorem 2). The black dashed line shows the average alignment to the input data, which is significantly weaker.

different initializations, different data transformations (controlled by the arbitrary matrix M), and different architectures (width and depth). This is only possible if the first layer transforms the representation into an input-independent form. See Figure 6 for a demonstration. This theorem is a direct (perhaps the first) proof of the platonic representation hypothesis, implying that for any x_1, x_2 , Eq. (5) holds. Importantly, the mechanism does not belong to any previously conjectured mechanisms (capacity, simplicity, multitasking (Huh et al., 2024)). This example has nothing to do with multitasking. The result holds for any deep linear network, all having the same capacity and the same level of simplicity because all solutions parametrize the same input-output map. Here, the cause of the universal representation is symmetry alone: in the degenerate manifold of solutions, the training algorithm prefers a particular and universal one. This example showcases how symmetry is indeed an overlooked fundamental mechanism in deep learning.

An important future step is to generalize it to nonlinear networks. Due to extensive connectivity among the global minima of overparametrized networks (Nguyen, 2019), there is a great potential that parameter symmetry (in exact or approximate forms) plays a similar role in overparameterized neural networks (Zhao et al., 2022, 2023a).

6 Mechanism and Control

Mechanism: A primary known mechanism is regularization in explicit or implicit forms. Since symmetry breaking is just the lack of symmetry restoration, we may focus on symmetry restoration. In explicit form, a simple weight decay has been shown to universally turn symmetric solutions energetically favorable to symmetry-broken solutions (Ziyin, 2024), in a manner similar to phase transition in physics (Landau & Lifshitz, 2013). In implicit form, the stochasticity in SGD is known to lead to an “implicit” regularization effect, sometimes similar to that of weight decay (Kunin et al., 2021; Chen et al., 2023). Another mechanism is data augmentation, as it can also be seen as a form of regularization (Dao et al., 2019). While understanding these mechanisms is an open problem, the easiest way to study it is to consider the effective loss landscape (also known as the “modified loss”) under SGD training (Geiping et al., 2021; Smith et al., 2021):

$$L(\theta) = \underbrace{\mathbb{E}_\epsilon[L_0(\theta, x_\epsilon)]}_{\text{learning + data aug.}} + \underbrace{\gamma\|\theta\|^2}_{\text{weight decay}} + \underbrace{T \text{Tr}[\Sigma(\theta)]}_{\text{training noise}}, \quad (7)$$

where L_0 has the symmetry under consideration, Σ is the gradient covariance matrix due to SGD sampling, and $T = \eta/S$ is the learning-rate-to-batch-size ratio. The data augmentation term can also be controlled by,

say, a variance term σ . A careful inspection suggests that none of these terms breaks the Z_2 symmetries of L_0 . So all σ , γ , T can serve as regularizers that can induce a “spontaneous symmetry breaking,” which means that the symmetric states are energetically favored solutions at a critical regularization strength (Ziyin, 2024). We experimentally demonstrate these effects in Section A.3.

With explicit regularization, whether symmetry breaking or restoration happens depends on the competition between regularization γ and the data signal. The more curious situation is when $\gamma = 0$ and $T > 0$. This type of symmetry breaking is more like a thermodynamic phase transition in physics as it is induced by an entropic force due to the SGD noise. Why do noisy dynamics favor symmetric states? One intuition is that the “temperature” of the dynamics is parameter-dependent, and stochastic dynamics tend to move to places that are “cold,” a common phenomenon in nature (Duhr & Braun, 2006; Anzini et al., 2019).¹ In other words, temperature gradient tends to create a flow. In the case of SGD dynamics on a neural network, the symmetric solutions are “colder” because they have a lower-rank Σ than the symmetry-broken solutions. This discussion offers a likely intuition for the mechanism, but a more formal treatment of the argument is still lacking. Different training techniques likely favor different types of symmetries, and one may leverage symmetry to understand the inductive biases of deep learning techniques.

Control: If hierarchies and complexity adaptivity are desired, one can introduce artificial symmetries to the neural network. A straightforward way to introduce symmetries is by introducing an additional parameter v and multiplying it with the parameters W for which a hierarchy is desired. For example, changing a layer weight from W to vW introduces a new symmetry without affecting the model expressivity: $|v| = \|W\| = 0$ is the symmetric state, and the model will naturally adapt to break or restore this symmetry. This is a special case of a class of algorithms that introduce artificial symmetries to constrain the model parameters. (for example, see the DCS algorithm in Ziyin (2024); also, see Kolb et al. (2025)). A simple way to remove symmetries is to add some static randomness to the model, which has been found to help with the model connectivity (Lim et al., 2024) and avoid saddle points (Ziyin et al., 2025b). Finding the right symmetries to introduce or remove can be a fruitful future direction.

7 Outlook and Alternative Views

In this work, we have argued and demonstrated that a wide range of seemingly unrelated hierarchies emergent in AI systems is actually related to, if not directly caused by, the symmetry of the trained models. Symmetry breaking and restoration are fundamental mechanisms in physics relevant to the dynamics of almost every scale of nature – from scattering of the quarks to the large-scale structure formation of the universe (Miller et al., 1990; Preskill et al., 1991). If different symmetries govern the universal laws at different scales of nature (Anderson, 1972), it is natural to hypothesize that it may also lead to universal mechanisms and laws of learning in both artificial and biological systems. We suggest three primary hypothetical mechanisms that govern three fundamental aspects of hierarchical learning of neural networks, and validating or falsifying their related hypotheses is the most important next step. From a broader perspective, that symmetry can play such important roles in learning also calls for more interdisciplinary study of intelligence from the perspective of physics.

There are certainly alternative views to our position.

Symmetry alone is insufficient: In most of our examples, it is a combination of symmetry and some other effect that leads to the phenomenon. For example, the compression bias of SGD is a result of symmetry *and* training noise. Neural collapse is due to symmetry *and* regularization (Rangamani & Banburski-Fahey, 2022). Therefore, it is possibly the case that symmetry *plus* some form of explicit (weight decay) or implicit (noise, GD training, data augmentation) regularization is the dominating factor, and this may be an important direction of future research.

Symmetry may not be necessary: While symmetry is possibly a unified perspective to view many phenomena, there are cases where a subset of these phenomena are exhibited but does not require symmetry. For theoretical purposes, this suggests that there can be other concepts as important as symmetry. However, from a design and practice perspective, knowing only one way to achieve a design goal often suffices – and the parameter symmetry may be sufficient. For example, there may be multiple ways for neural collapse to happen, but to introduce neural collapse to the desired model, one only needs to know one such way.

¹So, implicit regularization effects can be viewed as a thermal current obeying laws of nonequilibrium physics (Seifert, 2008).

Behind symmetry there may be more: There are also possible more fundamental mechanisms than symmetry, which can explain what happens with symmetry and what happens without it. One such example could be the topology of the system. In fact, in theoretical physics, symmetry is often regarded as a special case of topology (for example, the rank of the Fisher information can be a good the topological invariant). This makes it possible to generalize our arguments to a wider range of systems. Some works have explored the role of topology in AI, but often in a scenario where symmetry is also present (Barannikov et al., 2020; Nurisso et al., 2024). Another interesting future direction is understanding what topology may achieve without requiring symmetries.

Acknowledgment

ILC acknowledges support in part from the Institute for Artificial Intelligence and Fundamental Interactions (IAIFI) through NSF Grant No. PHY-2019786. This work was also supported by the Center for Brains, Minds and Machines (CBMM), funded by NSF STC award CCF - 1231216.

References

- Abbe, E., Adsera, E. B., and Misiakiewicz, T. Sgd learning on neural networks: leap complexity and saddle-to-saddle dynamics. In *The Thirty Sixth Annual Conference on Learning Theory*, pp. 2552–2623. PMLR, 2023.
- Alain, G. Understanding intermediate layers using linear classifier probes. *arXiv preprint arXiv:1610.01644*, 2016.
- Alain, G., Roux, N. L., and Manzagol, P.-A. Negative eigenvalues of the hessian in deep neural networks. *arXiv preprint arXiv:1902.02366*, 2019.
- Anderson, P. W. More is different: Broken symmetry and the nature of the hierarchical structure of science. *Science*, 177(4047):393–396, 1972.
- Andriopoulos, G., Dong, Z., Guo, L., Zhao, Z., and Ross, K. The prevalence of neural collapse in neural multivariate regression. *arXiv preprint arXiv:2409.04180*, 2024.
- Anzini, P., Colombo, G. M., Filiberti, Z., and Parola, A. Thermal forces from a microscopic perspective. *Physical Review Letters*, 123(2):028002, 2019.
- Bansal, Y., Nakkiran, P., and Barak, B. Revisiting model stitching to compare neural representations. *Advances in neural information processing systems*, 34:225–236, 2021.
- Barannikov, S., Voronkova, D., Trofimov, I., Korotin, A., Sotnikov, G., and Burnaev, E. Topological obstructions in neural networks learning. *arXiv preprint arXiv:2012.15834*, 2020.
- Bartlett, P. L., Harvey, N., Liaw, C., and Mehrabian, A. Nearly-tight vc-dimension and pseudodimension bounds for piecewise linear neural networks. *Journal of Machine Learning Research*, 20(63):1–17, 2019.
- Bengio, Y., Courville, A., and Vincent, P. Representation learning: A review and new perspectives. *IEEE transactions on pattern analysis and machine intelligence*, 35(8):1798–1828, 2013.
- Bronstein, M. M., Bruna, J., Cohen, T., and Velicković, P. Geometric deep learning: Grids, groups, graphs, geodesics, and gauges. *arXiv preprint arXiv:2104.13478*, 2021.
- Chen, F., Kunin, D., Yamamura, A., and Ganguli, S. Stochastic collapse: How gradient noise attracts sgd dynamics towards simpler subnetworks. *arXiv preprint arXiv:2306.04251*, 2023.
- Chizat, L., Oyallon, E., and Bach, F. On lazy training in differentiable programming. *arXiv preprint arXiv:1812.07956*, 2018.

- Cohen, J. M., Kaur, S., Li, Y., Kolter, J. Z., and Talwalkar, A. Gradient descent on neural networks typically occurs at the edge of stability. *arXiv preprint arXiv:2103.00065*, 2021.
- Dao, T., Gu, A., Ratner, A., Smith, V., De Sa, C., and Ré, C. A kernel theory of modern data augmentation. In *International conference on machine learning*, pp. 1528–1537. PMLR, 2019.
- Dinh, L., Pascanu, R., Bengio, S., and Bengio, Y. Sharp Minima Can Generalize For Deep Nets. *ArXiv e-prints*, March 2017.
- Dosovitskiy, A. An image is worth 16x16 words: Transformers for image recognition at scale. *arXiv preprint arXiv:2010.11929*, 2020.
- Du, S. S., Hu, W., and Lee, J. D. Algorithmic regularization in learning deep homogeneous models: Layers are automatically balanced. *Advances in neural information processing systems*, 31, 2018.
- Duhr, S. and Braun, D. Why molecules move along a temperature gradient. *Proceedings of the National Academy of Sciences*, 103(52):19678–19682, 2006.
- Entezari, R., Sedghi, H., Saukh, O., and Neyshabur, B. The role of permutation invariance in linear mode connectivity of neural networks. *arXiv preprint arXiv:2110.06296*, 2021.
- Feit, W. *The representation theory of finite groups*. Elsevier, 1982.
- Fok, R., An, A., and Wang, X. Spontaneous symmetry breaking in neural networks. *arXiv preprint arXiv:1710.06096*, 2017.
- Fukumizu, K. A regularity condition of the information matrix of a multilayer perceptron network. *Neural networks*, 9(5):871–879, 1996.
- Fukumizu, K. and Amari, S.-i. Local minima and plateaus in hierarchical structures of multilayer perceptrons. *Neural networks*, 13(3):317–327, 2000.
- Galanti, T., György, A., and Hutter, M. On the role of neural collapse in transfer learning. *arXiv preprint arXiv:2112.15121*, 2021.
- Galanti, T., Xu, M., Galanti, L., and Poggio, T. Norm-based generalization bounds for compositionally sparse neural networks. *arXiv preprint arXiv:2301.12033*, 2023.
- Geiping, J., Goldblum, M., Pope, P. E., Moeller, M., and Goldstein, T. Stochastic training is not necessary for generalization. *arXiv preprint arXiv:2109.14119*, 2021.
- Godfrey, C., Brown, D., Emerson, T., and Kvinge, H. On the symmetries of deep learning models and their internal representations. *Advances in Neural Information Processing Systems*, 35:11893–11905, 2022.
- Huh, M., Cheung, B., Wang, T., and Isola, P. The platonic representation hypothesis. *arXiv preprint arXiv:2405.07987*, 2024.
- Ioffe, S. and Szegedy, C. Batch normalization: Accelerating deep network training by reducing internal covariate shift. *arXiv preprint arXiv:1502.03167*, 2015.
- Jacot, A., Gabriel, F., and Hongler, C. Neural tangent kernel: Convergence and generalization in neural networks. *arXiv preprint arXiv:1806.07572*, 2018.
- Jacot, A., Ged, F., Şimşek, B., Hongler, C., and Gabriel, F. Saddle-to-saddle dynamics in deep linear networks: Small initialization training, symmetry, and sparsity. *arXiv preprint arXiv:2106.15933*, 2021.
- Kalimeris, D., Kaplun, G., Nakkiran, P., Edelman, B., Yang, T., Barak, B., and Zhang, H. Sgd on neural networks learns functions of increasing complexity. *Advances in neural information processing systems*, 32, 2019.
- Kobayashi, S., Akram, Y., and Von Oswald, J. Weight decay induces low-rank attention layers. *arXiv preprint arXiv:2410.23819*, 2024.

- Kolb, C., Weber, T., Bischl, B., and Rügamer, D. Deep weight factorization: Sparse learning through the lens of artificial symmetries, 2025.
- Kornblith, S., Norouzi, M., Lee, H., and Hinton, G. Similarity of neural network representations revisited. In *International conference on machine learning*, pp. 3519–3529. PMLR, 2019.
- Kunin, D., Sagastuy-Brena, J., Gillespie, L., Margalit, E., Tanaka, H., Ganguli, S., and Yamins, D. L. Rethinking the limiting dynamics of sgd: modified loss, phase space oscillations, and anomalous diffusion. 2021.
- Landau, L. D. and Lifshitz, E. M. *Statistical Physics: Volume 5*, volume 5. Elsevier, 2013.
- Li, S.-H. and Wang, L. Neural network renormalization group. *Physical review letters*, 121(26):260601, 2018.
- Li, X., Wang, Z., Lu, J., Arora, R., Haupt, J., Liu, H., and Zhao, T. Symmetry, saddle points, and global geometry of nonconvex matrix factorization. *arXiv preprint arXiv:1612.09296*, 1:5–1, 2016.
- Li, Z., Lyu, K., and Arora, S. Reconciling modern deep learning with traditional optimization analyses: The intrinsic learning rate. *Advances in Neural Information Processing Systems*, 33:14544–14555, 2020.
- Li, Z., Wang, T., and Arora, S. What happens after sgd reaches zero loss?—a mathematical framework. In *International Conference on Learning Representations*, 2021.
- Lim, D., Putterman, T. M., Walters, R., Maron, H., and Jegelka, S. The empirical impact of neural parameter symmetries, or lack thereof. *arXiv preprint arXiv:2405.20231*, 2024.
- Marcotte, S., Gribonval, R., and Peyré, G. Abide by the law and follow the flow: Conservation laws for gradient flows. 2023.
- Maron, H., Ben-Hamu, H., Shamir, N., and Lipman, Y. Invariant and equivariant graph networks. *arXiv preprint arXiv:1812.09902*, 2018.
- Masarczyk, W., Ostaszewski, M., Imani, E., Pascanu, R., Miłoś, P., and Trzcinski, T. The tunnel effect: Building data representations in deep neural networks. *Advances in Neural Information Processing Systems*, 36, 2024.
- Miller, G. A., Nefkens, B. M. K., and Šlaus, I. Charge symmetry, quarks and mesons. *Physics Reports*, 194(1-2):1–116, 1990.
- Mingard, C., Rees, H., Valle-Pérez, G., and Louis, A. A. Deep neural networks have an inbuilt occam’s razor. *Nature Communications*, 16(1):220, 2025.
- Neyshabur, B., Tomioka, R., and Srebro, N. In search of the real inductive bias: On the role of implicit regularization in deep learning. *arXiv preprint arXiv:1412.6614*, 2014.
- Neyshabur, B., Li, Z., Bhojanapalli, S., LeCun, Y., and Srebro, N. Towards understanding the role of over-parametrization in generalization of neural networks. *arXiv preprint arXiv:1805.12076*, 2018.
- Nguyen, Q. On connected sublevel sets in deep learning. In *International conference on machine learning*, pp. 4790–4799. PMLR, 2019.
- Nguyen, Q., Mukkamala, M. C., and Hein, M. Neural networks should be wide enough to learn disconnected decision regions. In *International conference on machine learning*, pp. 3740–3749. PMLR, 2018.
- Nurisso, M., Leroy, P., and Vaccarino, F. Topological obstruction to the training of shallow relu neural networks. *arXiv preprint arXiv:2410.14837*, 2024.
- Papayan, V., Han, X., and Donoho, D. L. Prevalence of neural collapse during the terminal phase of deep learning training. *Proceedings of the National Academy of Sciences*, 117(40):24652–24663, 2020.
- Peskin, M. E. *An introduction to quantum field theory*. CRC press, 2018.

- Pinto, A., Rangamani, A., and Poggio, T. On generalization bounds for neural networks with low rank layers. *arXiv preprint arXiv:2411.13733*, 2024.
- Preskill, J., Trivedi, S. P., Wilczek, F., and Wise, M. B. Cosmology and broken discrete symmetry. *Nuclear Physics B*, 363(1):207–220, 1991.
- Rangamani, A. and Banburski-Fahey, A. Neural collapse in deep homogeneous classifiers and the role of weight decay. In *ICASSP 2022-2022 IEEE International Conference on Acoustics, Speech and Signal Processing (ICASSP)*, pp. 4243–4247. IEEE, 2022.
- Rangamani, A., Lindegaard, M., Galanti, T., and Poggio, T. A. Feature learning in deep classifiers through intermediate neural collapse. In *International Conference on Machine Learning*, pp. 28729–28745. PMLR, 2023.
- Saxe, A. M., McClelland, J. L., and Ganguli, S. Exact solutions to the nonlinear dynamics of learning in deep linear neural networks. *arXiv preprint arXiv:1312.6120*, 2013.
- Seifert, U. Stochastic thermodynamics: principles and perspectives. *The European Physical Journal B*, 64(3-4):423–431, 2008.
- Simon, J. B., Knutins, M., Ziyin, L., Geisz, D., Fetterman, A. J., and Albrecht, J. On the stepwise nature of self-supervised learning. *arXiv preprint arXiv:2303.15438*, 2023.
- Simsek, B., Ged, F., Jacot, A., Spadaro, F., Hongler, C., Gerstner, W., and Brea, J. Geometry of the loss landscape in overparameterized neural networks: Symmetries and invariances. In *International Conference on Machine Learning*, pp. 9722–9732. PMLR, 2021.
- Smith, S. L., Dherin, B., Barrett, D. G., and De, S. On the origin of implicit regularization in stochastic gradient descent. *arXiv preprint arXiv:2101.12176*, 2021.
- Tanaka, H. and Kunitz, D. Noether’s learning dynamics: Role of symmetry breaking in neural networks. In Ranzato, M., Beygelzimer, A., Dauphin, Y., Liang, P., and Vaughan, J. W. (eds.), *Advances in Neural Information Processing Systems*, volume 34, pp. 25646–25660. Curran Associates, Inc., 2021. URL https://proceedings.neurips.cc/paper_files/paper/2021/file/d76d8deea9c19cc9aaf2237d2bf2f785-Paper.pdf.
- Tatro, N., Chen, P.-Y., Das, P., Melnyk, I., Sattigeri, P., and Lai, R. Optimizing mode connectivity via neuron alignment. *Advances in Neural Information Processing Systems*, 33:15300–15311, 2020.
- Tibshirani, R. J. Equivalences between sparse models and neural networks. *Working Notes*. URL <https://www.stat.cmu.edu/~ryantibs/papers/sparsitynn.pdf>, 2021.
- Tishby, N. and Zaslavsky, N. Deep learning and the information bottleneck principle. In *2015 IEEE Information Theory Workshop (ITW)*, pp. 1–5. IEEE, 2015.
- Tishby, N., Pereira, F. C., and Bialek, W. The information bottleneck method. *arXiv preprint physics/0004057*, 2000.
- Vaswani, A., Shazeer, N., Parmar, N., Uszkoreit, J., Jones, L., Gomez, A. N., Kaiser, Ł., and Polosukhin, I. Attention is all you need. *Advances in neural information processing systems*, 30, 2017.
- Watanabe, S. and Oppen, M. Asymptotic equivalence of bayes cross validation and widely applicable information criterion in singular learning theory. *Journal of machine learning research*, 11(12), 2010.
- Wu, R. and Pappas, V. Linguistic collapse: Neural collapse in (large) language models. *arXiv preprint arXiv:2405.17767*, 2024.
- Xu, M., Galanti, T., Rangamani, A., Rosasco, L., and Poggio, T. The janus effects of sgd vs gd: high noise and low rank. 2023.

- Yamins, D. L., Hong, H., Cadieu, C. F., Solomon, E. A., Seibert, D., and DiCarlo, J. J. Performance-optimized hierarchical models predict neural responses in higher visual cortex. *Proceedings of the national academy of sciences*, 111(23):8619–8624, 2014.
- Yang, G. and Hu, E. J. Feature learning in infinite-width neural networks. *arXiv preprint arXiv:2011.14522*, 2020.
- Zeiler, M. D. and Fergus, R. Visualizing and understanding convolutional networks. In *Computer Vision—ECCV 2014: 13th European Conference, Zurich, Switzerland, September 6–12, 2014, Proceedings, Part I 13*, pp. 818–833. Springer, 2014.
- Zhang, C., Bengio, S., Hardt, M., Recht, B., and Vinyals, O. Understanding deep learning requires rethinking generalization. 2017. URL <https://arxiv.org/abs/1611.03530>.
- Zhao, B., Dehmamy, N., Walters, R., and Yu, R. Symmetry teleportation for accelerated optimization. *Advances in Neural Information Processing Systems*, 35:16679–16690, 2022.
- Zhao, B., Dehmamy, N., Walters, R., and Yu, R. Understanding mode connectivity via parameter space symmetry. In *UniReps: the First Workshop on Unifying Representations in Neural Models*, 2023a.
- Zhao, B., Gower, R. M., Walters, R., and Yu, R. Improving convergence and generalization using parameter symmetries. *arXiv preprint arXiv:2305.13404*, 2023b.
- Zhu, L., Liu, C., Radhakrishnan, A., and Belkin, M. Quadratic models for understanding neural network dynamics. *arXiv preprint arXiv:2205.11787*, 2022.
- Ziyin, L. Symmetry induces structure and constraint of learning. In *Forty-first International Conference on Machine Learning*, 2024.
- Ziyin, L., Li, B., Galanti, T., and Ueda, M. The probabilistic stability of stochastic gradient descent, 2023.
- Ziyin, L., Wang, M., Li, H., and Wu, L. Parameter symmetry and noise equilibrium of stochastic gradient descent. In *The Thirty-eighth Annual Conference on Neural Information Processing Systems*, 2024.
- Ziyin, L., Chuang, I., Galanti, T., and Poggio, T. Formation of representations in neural networks. *International Conference on Learning Representations*, 2025a.
- Ziyin, L., Xu, Y., and Chuang, I. Remove symmetries to control model expressivity. *International Conference on Learning Representations*, 2025b.

A Experiments

A.1 Measurement of Δ^G

Permutation Symmetry For the permutation symmetry in fully connected layers, we have described the Δ^G for these pairwise symmetries. However, for a layer of width ψ , there are $O(\psi^2)$ many such pairs, but we do not have to care about every pair of these because, for most of our purposes, we only care about how many neurons are actually functional and how many neurons are useless. This fact can allow us to reduce the number of measurements to ψ . To achieve this, we first sort all the neurons according to the norm of the input and outgoing weights. Because for two neurons to become close, their norms also need to be close. Therefore, if two neurons have a large norm difference, their permutation symmetry must have been broken. Under this ordering, we measure the Δ^G for the pairs of neurons with the closest norms.

An alternative perspective to look at this is that these pairwise neuron distances form a generating set of the symmetric group, and we are counting the number of symmetry breaking of these subgroups generated by each generator.

Omission of G We will write Δ^G as Δ throughout the appendix because we are often comparing Δ for different groups and so the superscript G is different for most cases.

Double Rotation Symmetry Computing the degree of symmetry for the double rotation symmetry is rather tricky. In the ViT experiment (Figure 3), we measured the degree of symmetry in the self-attention layers. Here, the symmetry is the double rotation symmetry:

$$W_Q W_K = W_Q M M^{-1} W_K, \tag{8}$$

for an arbitrary invertible matrix M . The symmetric states are the ones where W_Q and W_K both become low-rank in the same subspace. Namely, it happens when there exists a vector n such that

$$W_Q n = 0, \quad W_K^T n = 0. \tag{9}$$

There are at most k such n where k is the right dimension of W_Q . This motivates this group’s following operational definition of Δ . We first compute the eigenvalue decomposition of $W_Q^T W_Q$ to obtain its eigenvectors U :

$$W_Q^T W_Q = U \Lambda_Q U^T. \tag{10}$$

We then compute the following matrix:

$$\Lambda_K = U^T W_K W_K^T U, \tag{11}$$

and the degree of symmetry is defined as

$$N_{\text{dos}} = \sum_i^k \mathbb{1}_{\Delta_i < \Delta_{\text{th}}}, \tag{12}$$

where

$$\Delta_i = |(\Lambda_Q)_{ii} - (\Lambda_K)_{ii}|. \tag{13}$$

Degree of Symmetry The *degree of symmetry* we compute is the number of all Δ^G such that $\Delta^G > \Delta_{\text{th}}^G$, where Δ_{th}^G is a certain threshold, often between 0.05 and 0.2. If this layer has h many neurons, we define

$$N_{\text{dosb}} = h - N_{\text{dos}}, \tag{14}$$

and by definition $N_{\text{dosb}} \geq 0$.

A.2 Learning Dynamics

In Figure 2, we use a teacher-student setting, where both the teacher and student are five-layer fully connected networks (FCNs) with 64 units per layer and tanh activation. The input and output dimensions are 10

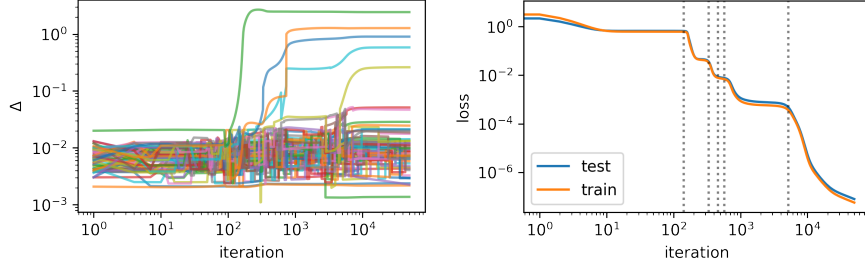


Figure 7: The same setting as Figure 2, but for quadratic activation. **Left:** Δ during training. **Right:** loss curve during training. Black dotted lines represent the time when Δ exceeds Δ_{th}^G .

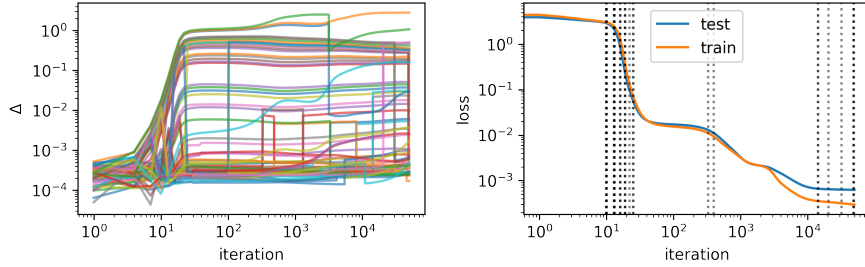


Figure 8: The same setting as Figure 2, but for sin activation.

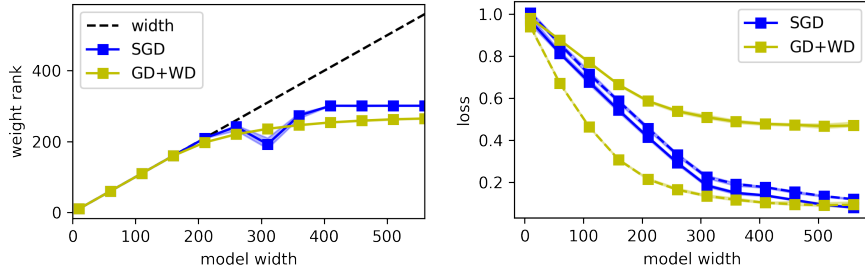


Figure 9: The same as Figure 3, and we report the rank of the first layer for completeness.

and 1, respectively. Teacher network weights follow Kaiming initialization, and the output is scaled by 10. The student network is initialized near zero. The training dataset consists of 300 samples generated as $\sin(\mathcal{N}(0, \sigma^2))$, with σ ranging from 0 to 3. The test dataset contains 500 samples from the same distribution. We train the student network with gradient descent (no weight decay) for 50,000 iterations using the mean squared error (MSE) loss.

To calculate the symmetry-breaking distance, we sort the first-layer neurons by their norms and compute the L_2 distance between consecutive neurons. Figure 2 shows distances for 63 neuron pairs in the first layer (see Section A.1). Results for quadratic and sin activations are presented in Figures 7 and 8.

A.3 Mechanisms for Symmetry Changes

For the left panel of Figure 3, we directly use the pretrained models of ViT-Base and ViT-Large from <https://pytorch.org/vision/stable/models.html>. The computation of the weight rank and N_{dosf} follows the outline in Section A.1.

In the middle panel of Figure 3, we train a three-layer fully connected network (FCN) with swish activation on a synthetic dataset where inputs and outputs are identical, sampled from a 300-dimensional standard Gaussian distribution. For gradient descent (GD), the dataset size is 1000, and weight decay is set to 10^{-3} . For stochastic gradient descent (SGD), the batch size is 128, with new data randomly generated for each

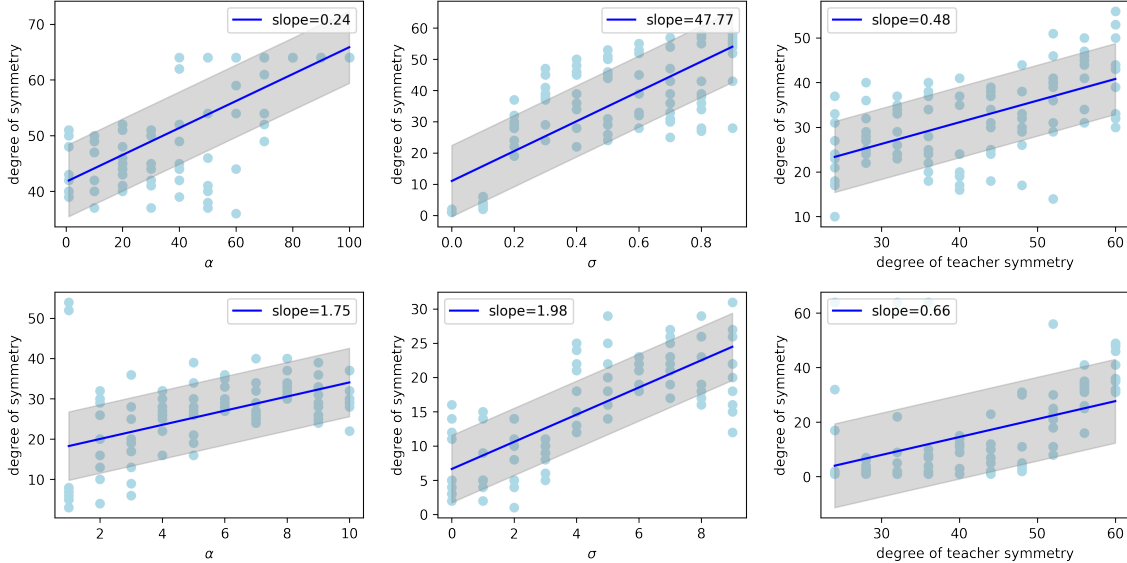


Figure 10: The degree of symmetry increases with α , the inverse scaling of input (**Left**), σ , the noise level (**Middle**), and the degree of teacher symmetry (64–the number of teacher units, **Right**). Blue dots represent experiment results, and blue lines represent linear fitting. **Upper**: MLP. **Lower**: transformer.

batch. In both cases, the test dataset contains 1000 samples, and the networks are trained using the Adam optimizer. For completeness, we report the rank of the first layer in Figure 9, which shows that both the rank and the generalization error remain constant when the model width gets larger.

In Figure 10, we analyze how symmetry evolves with input scaling, label noise, and the teacher symmetry. We adopt the teacher-student framework from Figure 2, using Gaussian inputs for the teacher network and the Adam optimizer with a weight decay of 10^{-2} . Symmetry is quantified as the number of first-layer neuron pair distances below 0.1 among 63 pairs in the student network. Teacher symmetry is measured as 64–the number of neurons in each teacher network layer. As expected, stronger noise, weaker inputs, or teachers with higher symmetry (simpler target functions) result in greater symmetry in the student network.

The second row of Figure 10 presents experiments on a simple transformer comprising two self-attention layers and one linear layer. We use an in-context learning dataset with input sequences of length 50, where each sequence element is a 21-dimensional token. The last dimension of each token is a linear combination of its first 20 dimensions, sampled from a standard Gaussian. The label corresponds to the last dimension of the final token in the sequence. The transformer is trained with the AdamW optimizer (weight decay 10^{-2}). The results for the transformer align with those for the MLP.

A.4 Neural Collapse

In Figure 4, we train ResNet18 on the CIFAR-10 dataset using vanilla weight decay and syre (Ziyin, 2024). In both cases, the weight decay is set to 5×10^{-4} . Networks are trained for 200 epochs, and results from the final epoch are reported. To generate Figure 4, we randomly select 10 images per class and compute the correlation between their features (i.e., the input to the final layer). The corresponding eigenvalue spectrum is presented in Figure 11, showing 10 prominent eigenvalues. Figures 12 and 13 extend these experiments with a weight decay of 5×10^{-3} , where the vanilla weight decay model exhibits a stronger low-rank structure compared to the syre model.

In Figure 5, we train a five-layer FCN with 512 neurons per layer and swish activation on CIFAR-10. Symmetry breaking is evaluated as the number of pairwise distances (as in Figure 2) exceeding 1. Results are averaged over 5 independent runs. Figure 14 replicates this experiment on the SVHN dataset, where the same hierarchical representation effects can be observed.

In Figure 6, we train two deep linear networks on MNIST using the Adam optimizer. Each network is a six-layer fully connected network (FCN) with 128 neurons per hidden layer. The average alignment to input

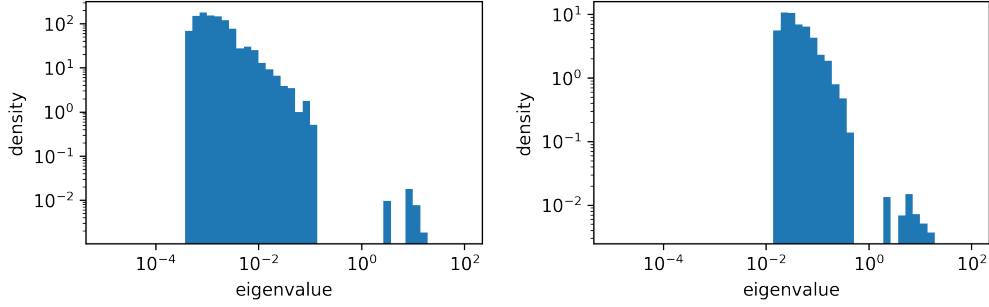


Figure 11: The spectrum of the representation correlation. **Left:** the vanilla model. **Right:** the syre model. While both models are low rank, the gaps between eigenvalues are smaller for the syre model.

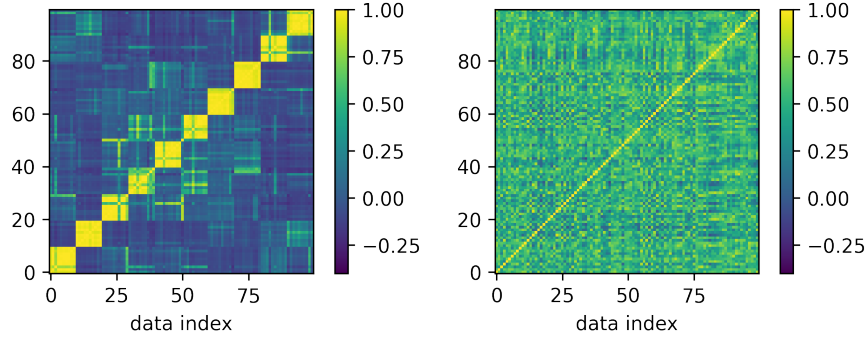


Figure 12: The same setting as Figure 4, but with weight decay ten times larger.

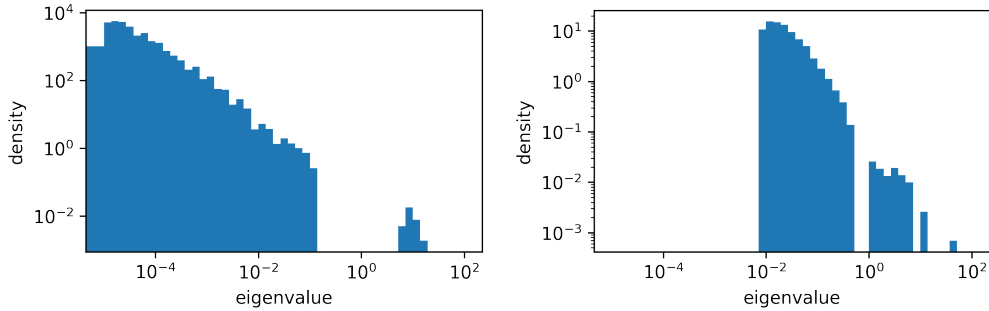


Figure 13: The same setting as Figure 11, but with weight decay ten times larger. The low-rank structure is largely suppressed.

data is computed as the average alignment between the data and the third layer during training. Figure 15 explores a similar setting for both linear and tanh networks, and the two networks have hidden layers with 64 and 128 neurons, respectively, where the universal alignment effects still hold.

A.5 Adaptive Capacity

In Figure 16, we train two-layer MLPs and simple transformers on synthetic datasets. The tasks match Figure 10, and we report the pairwise distances among six neurons. Figure 16 suggests that symmetry adapts to the training data in each run.

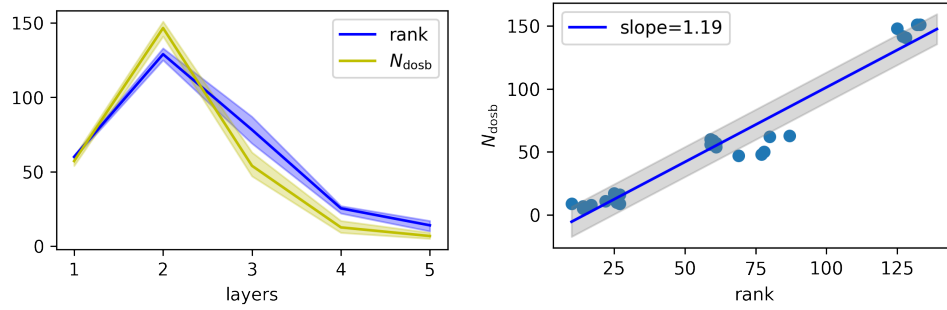


Figure 14: The same setting as Figure 5, but on the SVHN dataset.

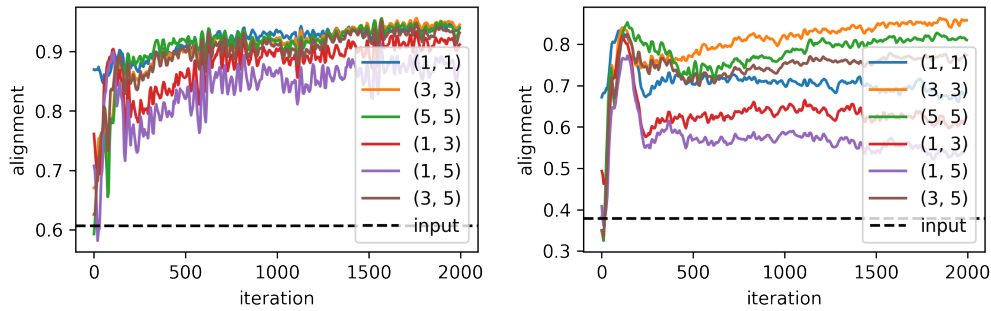


Figure 15: The raw data for Figure 6, but two networks have different number of neurons. The legend (i, j) denotes the alignment between the i -th layer of network A and the j -th layer of network B. **Left:** linear network. **Right:** tanh network.

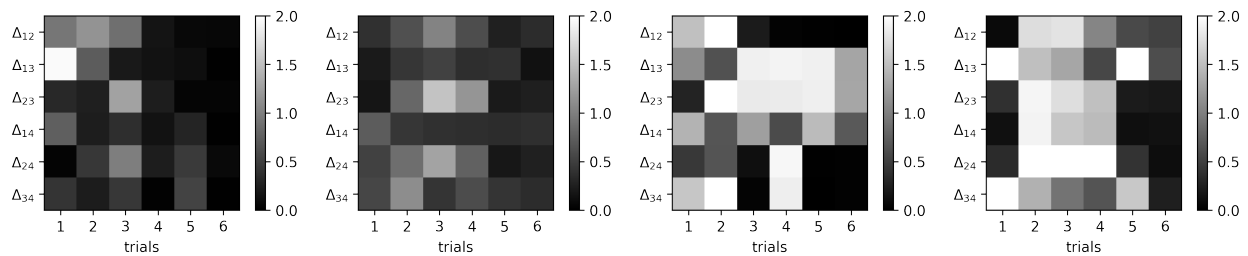


Figure 16: The final distance between the weights of neurons for different teachers and the same initialization. For different tasks, the model converged to a different symmetry class. Left to right: (1) MLP small init., (2) MLP large init., (3) transformer small init., (4) transformer large init.

B Theory

B.1 Formal Statement of Theorem 1

We consider the MSE loss for part 2 of the theorem.

$$\ell(x, \theta) = \|y(x) - f(x, \theta)\|^2. \quad (15)$$

Consider an empirical data distribution $P(x)$, where x contains both the input and the label. The SGD iteration is defined as

$$\theta_{t+1} = \theta_t - \eta \nabla_{\theta} \ell(x, \theta_t), \quad (16)$$

where $x \sim P(x)$ and η is the learning rate.

The GD iteration is defined as

$$\theta_{t+1} = \theta_t - \eta \nabla_{\theta} \mathbb{E}_{x \sim P(x)} [\ell(x, \theta_t)]. \quad (17)$$

Theorem 3. *Let f have the G -symmetry for which $P_G^T = P_G$, and θ be initialized at θ_0 such that $P_G \theta_0 = \theta_0$.*
 1. *For all time steps t under GD or SGD, there exists a model $f'(x, \theta')$ and sequence of parameters θ'_t such that for all x ,*

$$f'(x, \theta'_t) = f(x, \theta_t), \quad (18)$$

where $\dim(\theta') = \dim(P_G)$.

2. *The kernelized model, $g(x, \theta) = \lim_{\lambda \rightarrow 0} (\lambda^{-1} f(x, \lambda \theta + \theta_0) - f(x, \theta_0))$, converges to*

$$\theta^* = A^+ \sum_x \nabla_{\theta} f(x, \theta_0)^T y(x) \quad (19)$$

under GD for a sufficiently small learning rate. Here, $A := P_G \sum_x \nabla_{\theta} f(x, \theta_0)^T \nabla_{\theta} f(x, \theta_0) P_G$ and A^+ denotes the Moore–Penrose inverse of A .

The second part of the theorem means that in the kernel regime², being at a symmetric solution implies that the feature kernel features are being masked by the projection matrix $\nabla_{\theta} f(x, \theta_0) \rightarrow P_G \nabla_{\theta} f(x, \theta_0)$, and learning can only happen given these masks. The proof is a slight generalization of Propostions 2 and 3 in (Ziyin et al., 2025b).

Proof. 1. Note that ℓ has the G -symmetry when f has the G -symmetry. For $P_G \theta_0 = \theta_0$ and any θ , we have $\ell(x, \theta) = \ell(x, \theta_0 + P_G(\theta - \theta_0))$. Taking $\theta \rightarrow \theta_0$, we have

$$(I - P_G) \nabla_{\theta} \ell(x, \theta_0) = 0, \quad (20)$$

where we use $P_G^T = P_G$. Therefore, for $\theta_1 := \theta_0 + \eta \nabla_{\theta} \ell(x, \theta_0)$, we still have $P_G \theta_1 = \theta_1$.

As G is linear, we can suppose that $\{a_i\}_{i=1}^{\dim(P_G)}$ forms a basis of $\text{im}(P_G)$, and define $f'(x, \theta') := f(x, \sum_{i=1}^{\dim(V^G)} \theta'_i a_i)$ for $\dim(\theta') = \dim(P_G)$. By choosing $\theta'_i = \theta^T a_i$, we have $f'(x, \theta'_t) = f(x, \theta_t)$.

2. By (20), close to any symmetric point θ_0 (any θ_0 for which $P_G \theta_0 = \theta_0$), for all x , we have

$$f(x, \theta) - f(x, \theta_0) = \nabla_{\theta} f(x, \theta_0) P_G \Delta + O(\|\Delta\|^2). \quad (21)$$

Therefore, $g(x, \theta)$ simplifies to a kernel model

$$g(x, \theta) = \nabla_{\theta_0} f(x, \theta_0) P_G \theta. \quad (22)$$

Let us consider the squared loss $\ell(\theta) = \sum_x \|y(x) - g(x, \theta)\|^2$ and denote $A := \sum_x P_G \nabla_{\theta_0} f(x, \theta_0)^T \nabla_{\theta_0} f(x, \theta_0) P_G$, $b := P_G \sum_x \nabla_{\theta_0} f(x, \theta_0)^T y(x)$. The GD iteraiton is

$$\theta^{t+1} = \theta^t - 2\eta(A\theta^t - b), \quad (23)$$

²Technically, this is the lazy training limit (Chizat et al., 2018).

where $\theta^0 = 0$. If

$$\eta < \frac{1}{2\lambda_{\max}(A)}, \quad (24)$$

GD converges to

$$\begin{aligned} \theta^* &= \lim_{t \rightarrow \infty} \sum_{k=0}^t (I - 2\eta A)^k * 2\eta b \\ &= A^+ b, \end{aligned} \quad (25)$$

which is the standard least square solution. □

B.2 Formal Statement of Theorem 2

We will consider training a deep linear network with SGD and MSE loss

$$\ell(\theta, x) = \|W_D \cdots W_1 x - y(x)\|^2, \quad (26)$$

on datasets $\mathcal{D}_M = \{(Mx_i, y_i)\}_i$, where M is an invertible matrix, and $y_i = Vx_i + \epsilon_i$ for i.i.d. noise ϵ_i . We make the same assumptions as Theorem 5.4 of (Ziyin et al., 2024) (the most important of which is the SDE approximation to the SGD). Also, we use the definition of the noise equilibrium in (Ziyin, 2024), which essentially means that SGD reaches stationarity in the degenerate directions of the double rotation symmetry.

Theorem 4. *Let $V' = \sqrt{\Sigma_\epsilon} V \sqrt{\Sigma_x}$, $\text{rank}(V') = d$ and S' be a diagonal matrix containing singular values of V' . Consider two deep linear networks A and B with weights of arbitrary dimensions larger than d . Let model A train on \mathcal{D}_M and model B on $\mathcal{D}_{M'}$. Then, at the global minimum and at the noise equilibrium, every hidden layer of A is **perfectly** aligned with every hidden layer of B for any x , in the sense that*

$$h_A^{L_A}(x) = c_0 R h_B^{L_B}(x) \quad (27)$$

for $1 \leq L_A < D_A$ and $1 \leq L_B < D_B$ and any x , where $c_0 = \left(\frac{\text{Tr} S'}{d}\right)^{\frac{2L_A - D_A}{2D_A} - \frac{2L_B - D_B}{2D_B}}$ is a constant and $R = U_1 U_2^T$, satisfying $U_1^T U_1 = U_2^T U_2 = I_d$. $h_A^{L_A}(x) := \Pi_{i=1}^{L_A} W_i^A M x$, $h_B^{L_B}(x) := \Pi_{i=1}^{L_B} W_i^B M' x$ denote the output of the L_A, L_B -the layer of network A and B , respectively.

Proof. Let $V' := \tilde{U} S' \tilde{V}$ be its SVD. According to Theorem 5.4 of (Ziyin et al., 2024). At the global minimum and noise equilibrium under SGD, the solution of a D_A -layer network for the dataset \mathcal{D}_M is given by

$$\sqrt{\Sigma_\epsilon} M_2 W_{D_A}^A = \tilde{U} \Sigma_D U_{D_A-1}^T, \quad W_i^A = U_i \Sigma_i U_{i-1}^T, \quad W_1^A M_1 \sqrt{\Sigma_x} = U_1 \Sigma_1 \tilde{V} \quad (28)$$

for $i = 2, \dots, D-1$, where U_i are arbitrary matrices satisfying $U_i^T U_i = I_{d \times d}$, and

$$\Sigma_1 = \Sigma_D = \left(\frac{d}{\text{Tr} S'}\right)^{(D_A-2)/2D_A} \sqrt{S'}, \quad \Sigma_i = \left(\frac{\text{Tr} S'}{d}\right)^{1/D_A} I_{d \times d}. \quad (29)$$

We can verify that $\Pi_{i=1}^{D_A} W_i^A M = V$, or $h_A^{D_A}(x) = Vx$ as expected. The solution suggests that

$$\Pi_{i=1}^{L_A} W_i^A M = U_{L_A} \left(\frac{\text{Tr} S'}{d}\right)^{\frac{2L_A - D_A}{2D_A}} \sqrt{S'} \tilde{V}. \quad (30)$$

Similarly

$$\Pi_{i=1}^{L_B} W_i^B M' = U_{L_B} \left(\frac{\text{Tr} S'}{d}\right)^{\frac{2L_B - D_B}{2D_B}} \sqrt{S'} \tilde{V}. \quad (31)$$

The proof is complete by comparing (30) and (31). □

B.3 Space Quantization Conjecture

Theorem 5. Consider the loss $\ell(\theta) = \ell_0(\theta) + \gamma\|\theta\|^2$ with $\theta := (\theta_1, \dots, \theta_k)$ and $\theta_i \in \mathbb{R}^n$ for $1 \leq i \leq k$. Assume that $\ell_0(\theta_1, \dots, \theta_k)$ has the permutation symmetry $\ell_0(\theta_1, \dots, \theta_i, \dots, \theta_j, \dots, \theta_k) = \ell_0(\theta_1, \dots, \theta_j, \dots, \theta_i, \dots, \theta_k)$ for any $1 \leq i, j \leq k$ and satisfies the following q -Lipschitz condition

$$\|\nabla \ell_0(\theta) - \nabla \ell_0(\theta')\| \leq K\|\theta - \theta'\|^q \quad (32)$$

for $q \geq 1$. Moreover, assume that $\inf_{\theta} \ell_0(\theta) > -\infty$ and that K scales with the number of active neurons m as $K = K_0 m^{-\alpha}$. Then, at any global minimum,

$$m \leq C\gamma^{-\frac{q+1}{2\alpha}} \quad (33)$$

for n large enough, where C is some constant.

Proof. We first consider two vectors $\theta_1 \neq \theta_2$. Suppose that the global minimum is at $\ell(\theta_1, \theta_2)$. We would like to compare the loss between (θ_1, θ_2) and $(\frac{1}{2}(\theta_1 + \theta_2), \frac{1}{2}(\theta_1 + \theta_2))$, which gives

$$\begin{aligned} & \ell(\theta_1, \theta_2) - \ell\left(\frac{1}{2}(\theta_1 + \theta_2), \frac{1}{2}(\theta_1 + \theta_2)\right) \\ &= \ell_0(\theta_1, \theta_2) - \ell_0\left(\frac{1}{2}(\theta_1 + \theta_2), \frac{1}{2}(\theta_1 + \theta_2)\right) + \gamma(\|\theta_1\|^2 + \gamma\|\theta_2\|^2 - 2\gamma\|\frac{1}{2}(\theta_1 + \theta_2)\|^2) \\ &= \ell_0(\theta_1, \theta_2) - \ell_0\left(\frac{1}{2}(\theta_1 + \theta_2), \frac{1}{2}(\theta_1 + \theta_2)\right) + \frac{1}{2}\gamma\|\theta_1 - \theta_2\|^2. \end{aligned} \quad (34)$$

For the first term, we have

$$\|\ell_0(\theta_1, \theta_2) - \ell_0\left(\frac{1}{2}(\theta_1 + \theta_2), \frac{1}{2}(\theta_1 + \theta_2)\right)\| \leq \|\theta_1 - \theta_2\| \max_{z \in [0,1]} |f'(z)| \|\theta_1 - \theta_2\|, \quad (35)$$

where

$$f(z) := \ell_0\left(\frac{1}{2}(\theta_1 + \theta_2) + z(\theta_1 - \theta_2), \frac{1}{2}(\theta_1 + \theta_2) - z(\theta_1 - \theta_2)\right). \quad (36)$$

By permutation symmetry, we have

$$f'(0) = \left(\nabla_1 \ell_0\left(\frac{1}{2}(\theta_1 + \theta_2), \frac{1}{2}(\theta_1 + \theta_2)\right) - \nabla_2 \ell_0\left(\frac{1}{2}(\theta_1 + \theta_2), \frac{1}{2}(\theta_1 + \theta_2)\right)\right)^T (\theta_1 - \theta_2), \quad (37)$$

where ∇_1 and ∇_2 denote the derivative of ℓ_0 w.r.t. its first and second variable. By the permutation symmetry, we have $\nabla_1 \ell_0\left(\frac{1}{2}(\theta_1 + \theta_2), \frac{1}{2}(\theta_1 + \theta_2)\right) = \nabla_2 \ell_0\left(\frac{1}{2}(\theta_1 + \theta_2), \frac{1}{2}(\theta_1 + \theta_2)\right)$, and thus $f'(0) = 0$.

As $\nabla \ell_0$ is q -Lipschitz, we have

$$f'(z) \leq Kz^q \|\theta_1 - \theta_2\|^q, \quad (38)$$

which gives

$$0 \geq \ell(\theta_1, \theta_2) - \ell\left(\frac{1}{2}(\theta_1 + \theta_2), \frac{1}{2}(\theta_1 + \theta_2)\right) \geq -K\|\theta_1 - \theta_2\|^{q+1} + \frac{1}{2}\gamma\|\theta_1 - \theta_2\|^2. \quad (39)$$

for the global minimum $\ell(\theta_1, \theta_2)$. Thus we have

$$\|\theta_1 - \theta_2\| \geq \left(\frac{\gamma}{2K}\right)^{1/(q-1)} \quad (40)$$

for $q > 1$. We conclude that any two vectors should be separated by a distance at least $\left(\frac{\gamma}{2K}\right)^{1/(q-1)}$.

Meanwhile, we have

$$\ell_0(\theta) + \gamma\|\theta\|^2 \leq \ell_0(0), \quad (41)$$

which gives

$$\|\theta_i\|^2 \leq \frac{\ell_0(0) - L^*}{\gamma}, \quad (42)$$

for $1 \leq i \leq k$, where $L^* = \inf_{\theta} \ell_0(\theta) > -\infty$.

Therefore, the problem is to put m points in a n -dimensional ball of radius $\sqrt{\frac{\ell_0(0) - L^*}{\gamma}}$, with pair-wise distance greater than $(\frac{\gamma}{2K})^{1/(q-1)}$. Thus we have

$$m \leq 2^n \left(\frac{\ell_0(0) - L^*}{\gamma} \right)^{n/2} \left(\frac{\gamma}{2K} \right)^{-n/(q-1)} = C' m^{-\frac{\alpha n}{q-1}} \gamma^{-\frac{q+1}{2(q-1)}n}, \quad (43)$$

which gives

$$m \leq C \gamma^{-\frac{q+1}{2\alpha} + O(1/n)}, \quad (44)$$

where C, C' denote some constants.

For $q = 1$, (39) gives

$$K_0 m^{-\alpha} - \frac{1}{2} \gamma \geq 0, \quad (45)$$

and thus

$$m \leq \left(\frac{\gamma}{2K_0} \right)^{-\frac{1}{\alpha}}. \quad (46)$$

□